Article

An Attempt to Observe Vertical Land Motion along the Norwegian Coast by CryoSat-2 and Tide Gauges

Martina Idžanović [1,*](ID), Christian Gerlach [1,2], Kristian Breili [1,3] and Ole Baltazar Andersen [4]

[1] Faculty of Science and Technology, Norwegian University of Life Sciences (NMBU), P.O. Box 5003, 1432 Ås, Norway; gerlach@badw.de (C.G.); kristian.breili@kartverket.no (K.B.)
[2] Geodesy and Glaciology, Bavarian Academy of Sciences and Humanities (BAdW), 80539 Munich, Germany
[3] Norwegian Mapping Authority (NMA), 3507 Hønefoss, Norway
[4] DTU Space, Technical University of Denmark, 2800 Kgs. Lyngby, Denmark; oa@space.dtu.dk
[*] Correspondence: maid@nmbu.no; Tel.: +47-672-316-04

Abstract: Present-day climate-change-related ice-melting induces elastic glacial isostatic adjustment (GIA) effects, while paleo-GIA effects describe the ongoing viscous response to the melting of late-Pleistocene ice sheets. The unloading initiated an uplift of the crust close to the centers of former ice sheets. Today, vertical land motion (VLM) rates in Fennoscandia reach values up to around 10 mm/year and are dominated by GIA. Uplift signals from GIA can be computed by solving the sea-level equation (SLE), $\dot{S} = \dot{N} - \dot{U}$. All three quantities can also be determined from geodetic observations: relative sea-level variations ($\dot{S}$) are observed by means of tide gauges, while rates of absolute sea-level change ($\dot{N}$) can be observed by satellite altimetry; rates of VLM ($\dot{U}$) can be determined by GPS (Global Positioning System). Based on the SLE, $\dot{U}$ can be derived by combining sea-surface measurements from satellite altimetry and relative sea-level records from tide gauges. In the present study, we have combined 7.5 years of CryoSat-2 satellite altimetry and tide-gauge data to estimate linear VLM rates at 20 tide gauges along the Norwegian coast. Thereby, we made use of monthly averaged tide-gauge data from PSMSL (Permanent Service for Mean Sea Level) and a high-frequency tide-gauge data set with 10-min sampling rate from NMA (Norwegian Mapping Authority). To validate our VLM estimates, we have compared them with the independent semi-empirical land-uplift model NKG2016LU_abs for the Nordic-Baltic region, which is based on GPS, levelling, and geodynamical modeling. Estimated VLM rates from 1 Hz CryoSat-2 and high-frequency tide-gauge data reflect well the amplitude of coastal VLM as provided by NKG2016LU_abs. We find a coastal average of 2.4 mm/year (average over all tide gauges), while NKG2016LU_abs suggests 2.8 mm/year; the spatial correlation is 0.58.

Keywords: CryoSat-2; tide gauges; Norwegian coast; vertical land motion; land-uplift model

1. Introduction

Vertical land motion (VLM) and changing sea levels result from a complex interplay of thermal expansion of ocean water, changing ice reservoirs, glacial isostatic adjustment (GIA), tectonic motion, and anthropogenic effects [1]. VLM is a key for understanding long-term relative sea-level changes, and, in Fennoscandia, it is dominated by GIA. The present effect of GIA reaches values of up to 10 mm/year in the Gulf of Bothnia (center of former ice sheet) and decreases to nearly zero at the edges of the former ice sheet. Uplift signals from GIA can be computed by solving the sea-level equation (SLE): $\dot{S} = \dot{N} - \dot{U}$. All three quantities of the SLE can be determined directly by time-series analysis of geodetic observations. Tide-gauge records constrain the relative sea-level change ($\dot{S}$), which is the variation of the sea surface relative to the solid Earth [1]. Tide gauges are attached to the Earth's crust making their measurements affected by VLM. On the other hand, satellite altimetry and GPS

(Global Positioning System) provide independent measurements of sea-level change $\dot{N}$ and VLM $\dot{U}$, respecively, with respect to a global geocentric reference frame. Based on the SLE, the combination of sea-surface measurements from altimetry and relative sea-level records from tide gauges can be used to isolate the VLM component $\dot{U}$ [2]. This method has been applied in previous studies, using point observations or gridded sea-level anomalies from conventional altimetry (e.g., Kuo et al. [1], Nerem and Mitchum [2], Pfeffer and Allemand [3]).

Nerem and Mitchum [2] used a ∼7.5 years long time series of observations from TOPEX/POSEIDON (T/P) (with 10-days sampling interval) in combination with (daily averaged) measurements from 114 globally distributed tide gauges to compute VLM. The mean total error of the VLM estimates was 2.6 mm/year. Fenoglio-Marc et al. [4] estimated VLM from T/P (1993–2001) and de-seasoned monthly tide-gauge data at 24 tide gauges in the Mediterranean Sea, which passed predefined selection criteria. Accounting for the serial correlation, the mean uncertainty of rates was 2.3 mm/year. Kuo et al. [1] also combined T/P altimetry data from 1992 to 2001 with monthly averaged tide-gauge records at 25 sites in the Baltic Sea region. The estimated VLM rates ranged from −7.5 to 13.4 mm/year and had an average uncertainty of 4.6 mm/year. The average uncertainty of VLM rates was significantly reduced to 0.4 mm/year by applying a network adjustment algorithm. The algorithm exploited long-term (>40 years) tide-gauge records to link relative VLM between all the involved tide gauges. The application of this approach is only possible in areas with long tide-gauge records available. An improved algorithm was used by Kuo et al. [5], which presented a VLM solution for Fennoscandia, with an average uncertainty of 0.5 mm/year. Ostanciaux et al. [6] combined 16 years of T/P, Jason-1, and Jason-2 data with annual tide-gauge records at 641 globally distributed sites including 64 sites in Fennoscandia south of 66°N. At those sites, the VLM rates ranged from −12.8 to 11.3 mm/year, with an average VLM rate of 1.6 mm/year. Pfeffer and Allemand [3] combined 20 years (1992–2013) of monthly averaged sea-level anomalies from a multi-satellite altimetry grid and monthly tide-gauge observations to evaluate VLM rates. Uncertainties of VLM rates ranged from 0.3 to 7.4 mm/year, with a mean uncertainty of 0.9 mm/year. Breili et al. [7] compared sea-level rates from two sets of altimetry data (1993–2016) along the Norwegian coast with sea-level rates estimated from 19 tide-gauge records corrected for VLM. The coastal averages of the sea-level rates were within errors, indicating that no systematic errors are present in the observations nor in the applied corrections.

In this study, we explore the potential of using tide-gauge observations in combination with data from the European Space Agency (ESA) CryoSat-2 (CS2) [8] to calculate VLM rates at 20 tide gauges along the Norwegian coast. The CS2 data have several advantages we will benefit from when combining it with tide-gauge observations. First, due to the orbit configuration of CS2, areas north of 66°N are covered by observations and its 369-days repeat orbit implies dense sampling of the ocean. Furthermore, CS2 has a synthetic aperture interferometric radar altimeter (SIRAL) that can be operated in three modes: low resolution, synthetic aperture radar (SAR), and interferometric SAR (SARIn). In SAR and SARIn modes, the footprint in the along-track direction is ∼300 m, in contrast to ∼8 km in the low-resolution mode. Smaller footprints reduce the risk of data contaminated by back-scattered energy from land features in the coastal zones, and allow the sea-surface height to be sampled closer to land. As a result of this, CS2 SARIn observations are available in a zone stretching out ∼40 km off the coast [9] (see Figure 1b), opposed to conventional altimetry that provides observation points, which are on average ∼54 km from the Norwegian tide gauges [10] and need to be extrapolated towards the coast. Our results will be compared to independent VLM rates from a land-uplift model based on GPS, levelling, and geophysical modeling. We will test the existence of systematic errors in our results and investigate whether CS2 in combination with tide-gauge data is able to sample the spatial variation in VLM along the Norwegian coast. In addition to providing new estimates of VLM at Norwegian tide gauges, the present study demonstrates the coastal accuracy of CS2 data and its retracker.

Section 2 describes data and methods used to determine VLM rates. Section 2.4 presents data used to validate our VLM rates, i.e., the absolute land-uplift model for the Nordic-Baltic region

NKG2016LU_abs [11]. Comparison results are shown in Section 3. Finally, we discuss our results and give concluding remarks in Section 4.
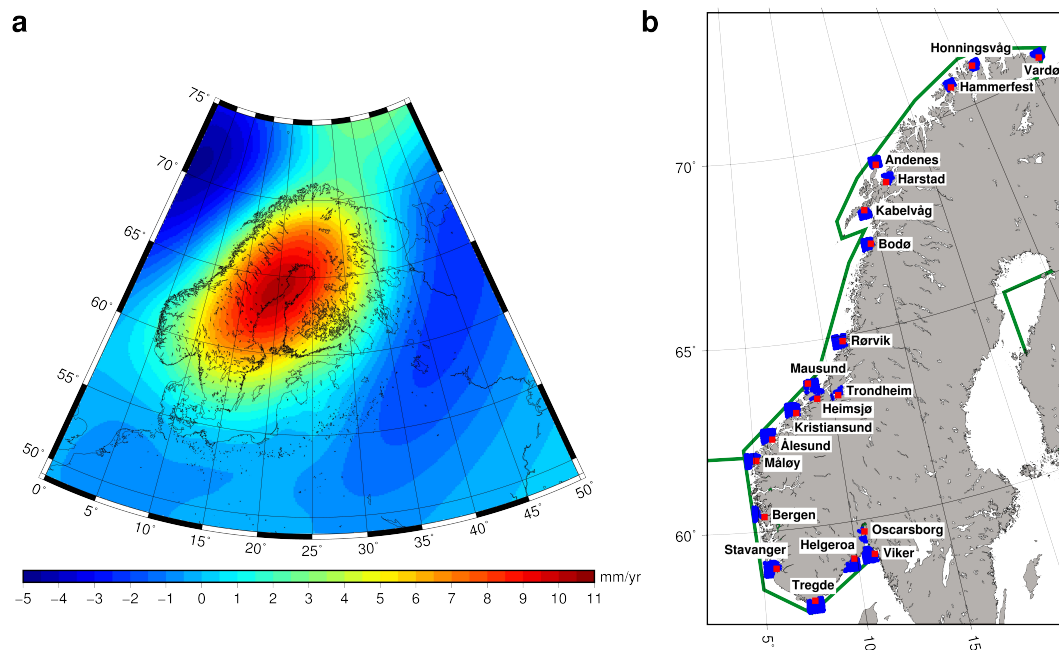
a

b

Figure 1. (**a**) The absolute land-uplift model for the Nordic-Baltic region NKG2016LU_abs [11] in ITRF2008. (**b**) Blue dots indicate available CS2 SARIn observations in 45 km × 45 km CS2 boxes around 20 Norwegian tide gauges. Red squares indicate the tide-gauge locations (see Supplementary Materials Table S1). The green line shows the CS2 SARIn-mode border, using the geographical mode mask version 3.9 [12].

2. Data and Methods

2.1. CryoSat-2 SARIn Data Processing

In this study, CS2 SARIn sea-level anomalies were obtained from the ESA Grid Processing on Demand (GPOD) service [13]. We used 1 and 20 Hz Level-2 products derived from the CS2 Level-1B products in SARIn mode for the period between July 2010 and December 2017. Three processing stages were included in the downloaded data set: reprocessing (RPRO), off-line routine operations (OFFL), and long-term archive (LTA). The SAR Altimetry Mode Studies and Applications (SAMOSA) 2 physical retracker [14] was applied as well as the SARIn off-nadir range correction [15,16]. The downloaded CS2 sea-level anomalies were computed with respect to the DTU15 mean sea surface (MSS) [17], and corrected for dry and wet tropospheric refraction, ionospheric delay computed from the global ionospheric model [18], ocean tides provided by the FES2004 model [19], long-period ocean tides, ocean-tide loading, solid Earth tides, pole tides, and dynamic atmosphere correction (DAC). The DAC consisted of a high-frequency part that is provided by MOG2D [20] and a low-frequency part, inverted barometer (IB), provided by the European Centre for Medium-Range Weather Forecasts (ECMWF) [21]. The sea state bias correction was not available.

No a priori data editing or quality assessment has been applied to the downloaded SARIn data. Therefore, we first removed all observations over land applying a land mask. Secondly, observations flagged as contaminated echoes or unclear ocean signals were rejected. The LTA data covered a time span between July 2010 and February 2015, OFFL from May 2012 until December 2017, and RPRO from July 2010 to January 2012. For the period before August 2013, there were some LTA observations that had epochs identical to observation epochs in the RPRO and OFFL data sets. Mean sea-level anomaly (SLA) differences for the overlapping time stamps were less than 0.2 cm. To avoid epochs with duplicated observations, we eliminated LTA observations for these time stamps.

Next, we rejected all |SLA| > 1 m. To identify and eliminate outliers, we used the same approach as outlined in Idžanović et al. [22]. With this method, the multiple Student's *t* test [23] was applied to the sea-level anomalies in each individual satellite pass. In the last step, we established 45 km × 45 km boxes around each tide gauge containing CS2 observations and formed "CS2 tide gauges", see Figures 1b and 2. The positions and dimension of the CS2 boxes are equivalent to those defined in Idžanović et al. [22]. Using the 20 Hz CS2 data, we have significantly more CS2 observations available in our CS2 boxes (see Table 1), and can gain a few kilometers towards the tide gauges. Therefore, we used both 1 and 20 Hz data to determine VLM rates.
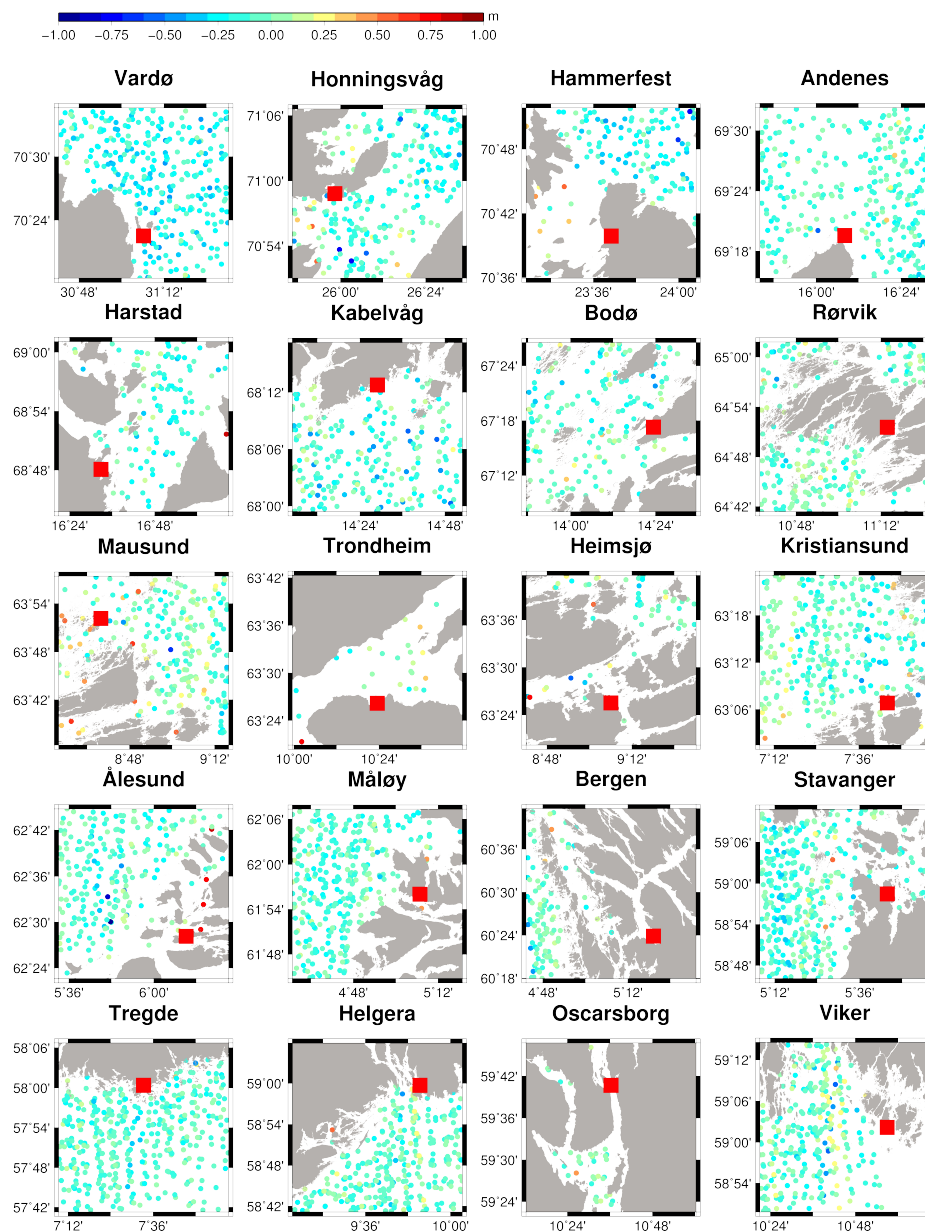

Figure 2. 1 Hz CS2 SARIn sea-level anomalies around 20 Norwegian tide gauges in 45 km × 45 km CS2 boxes. Red squares indicate the tide-gauge locations.

2.2. Tide-Gauge Data

There are in total 23 tide gauges along the Norwegian coast. The tide gauges in Tromsø, Narvik, and Oslo are located inside fjords and do not have enough CS2 observations available for trend computations. Thus, we used a subset of 20 tide gauges to estimate VLM rates (see Figure 1b and Supplementary Materials Table S1). Two tide-gauge data sets were used in this study: (i) monthly

averaged sea-level observations obtained from the Permanent Service for Mean Sea Level (PSMSL) [24] at http://www.psmsl.org/data/obtaining/ and (ii) 10-min sea-level observations obtained from the database of the Norwegian Mapping Authority (NMA). Both data sets cover the same period as the CS2 observations, i.e., from 2010 to 2018. The NMA tide-gauge data are given as observed water levels referred to tide-gauge zero. To each tide-gauge record from NMA, ocean-tide (OT) corrections were applied. These corrections were estimated in a harmonic analysis of several years of water-level observations from the current tide gauge. OT corrections were not applied to PSMSL observations since the strongest tidal constituents will be close to zero in monthly averages of tide-gauge observations [3,4]. The IB corrections were applied to neither PSMSL nor NMA tide-gauge records. At the tide gauge in Mausund, monthly sea-level observations are not available in the archives of PSMSL. Thus, monthly averages were computed from the NMA record with 10-min sampling interval instead. For consistency between altimetry and tide-gauge data sets, the DAC correction provided by GPOD was added back to the sea-level anomalies, meaning that the CS2 observations were not corrected for DAC [1].

2.3. Rates of Vertical Land Motion

The PSMSL and NMA tide-gauge data were interpolated using nearest-neighbor interpolation onto 1 and 20 Hz time stamps of CS2 SARIn observations. VLM rates and standard deviations of residuals, s_e, were then computed by fitting a linear regression model to the differences. To account for serial correlation in the time series, final rate uncertainties (σ) were estimated by:

$$\sigma = s_e \sqrt{\frac{1 + r^1}{1 - r^1}}, \tag{1}$$

where r^1 is the lag-1 autocorrelation coefficient computed from the residuals of the regression [25]. In the following, $VLM_{1HzPSMSL}$ and VLM_{1HzNMA} refer to VLM rates estimated from tide-gauge observations from PSMSL and NMA, respectively, and 1 Hz CS2 data. Similarly, $VLM_{20HzPSMSL}$ and $VLM_{20HzNMA}$ are calculated from 20 Hz CS2 observations.

2.4. Validation Data

We used the absolute land-uplift model NKG2016LU_abs [11] for the Nordic-Baltic region to validate our calculated VLM rates. NKG2016LU_abs is a semi-empirical land-uplift model, which combines an empirical land-uplift model with a GIA model. The empirical model is based on BIFROST (Baseline Inferences for Fennoscandian Rebound Observations, Sea Level, and Tectonics) GPS velocities [26] and levelling, and does not include sea-level data. In the first step, estimates of vertical velocities were derived from GPS and levelling at the corresponding observation sites over land. In the next step, residuals with respect to vertical velocities derived from a GIA model were formed. These residuals were filtered and gridded by least-squares collocation, thus reducing the noise of the geodetic observations. In the final step, velocities of the GIA model were restored, yielding a smooth gridded surface representation of present-day VLM. The underlying GIA model, NKG2016GIA_prel0306, was computed applying the ICEAGE software [27]. This model uses a three-layered rheology and a thermo-mechanical ice history for Fennoscandia and the Barents Sea compiled by L. Tarasov [11]. The uncertainty of the VLM rates from NKG2016LU_abs was calculated to 0.6 mm/year by Olsson et al. [28], taking into account internal uncertainty (0.2 mm/year), as well as drift in the ITRF2008 reference frame's origin (0.5 mm/year) and scale (0.3 mm/year). Notice that the land-uplift model provides both (i) absolute land-uplift rates in ITRF2008 (NKG2016LU_abs, Figure 1a) and (ii) levelled land-uplift rates relative to the geoid (NKG2016LU_lev). In the following, when referring in the text to the NKG uplift model, the absolute land-uplift model NKG2016LU_abs is meant.

3. Results

Table 1 gives an overview of the amount of available 1 and 20 Hz CS2 SARIn observations within CS2 boxes as well as the mean difference and mean correlation between CS2 and tide-gauge time series computed over 20 Norwegian tide gauges. Generally, both 1 and 20 Hz CS2 time series agree well with the NMA tide-gauge time series. Averaged over all tide gauges, the 1 Hz CS2 time series show a standard deviation of differences and correlation of 11.9 cm and 0.82, respectively. The 20 Hz CS2 time series show a standard deviation of 12.1 cm and a correlation of 0.77. The agreement between 1 and 20 Hz CS2 time series with PSMSL is poorer. The 1 Hz CS2 time series show a standard deviation of 17.5 cm and a correlation of 0.53, while the 20 Hz time series show a standard deviation and correlation of 16.7 cm and 0.50, respectively. Hence, the tide-gauge time series from both NMA and PSMSL agree better with 1 Hz CS2 time series than with 20 Hz time series in terms of mean correlations.

Linear rates as well as associated uncertainties of VLM from the NKG uplift model and CS2 combined with tide-gauge records over the period 2010–2018 are illustrated in Figure 3. The upper and lower panels show VLM rates based on 1 and 20 Hz CS2 time series, respectively. The NKG land-uplift model shows positive rates (from 1.3 mm/year at Måløy to 4.7 mm/year at Trondheim) for all 20 tide gauges. This is also confirmed by the majority of our estimated VLM rates. The rate uncertainties calculated by Equation (1) take into account serial correlations of measurements. The uncertainties range from 3.1 to 27.1 mm/year when using 1 Hz CS2 sea-level anomalies and from 1.1 to 18.5 mm/year when using 20 Hz CS2 data. Largest uncertainties occur at tide gauges with few CS2 observations available, i.e., at Trondheim, Heimsjø, Oscarsborg, and Hammerfest (see Figure 2).

Table 2 lists key numbers from the comparison between our VLM estimates and rates from the NKG uplift model. VLM rates based on both 1 and 20 Hz CS2 data in combination with NMA tide-gauge measurements (VLM_{1HzNMA} and $VLM_{20HzNMA}$) agree with the NKG uplift model within uncertainties for most of the sites. Their differences range from -13.9 to 8.1 mm/year. When using PSMSL tide-gauge data for the VLM estimation ($VLM_{1HzPSMSL}$ and $VLM_{20HzPSMSL}$), differences range between -23.2 and 16.3 mm/year. The standard deviations of differences between the NKG uplift model and rates of VLM based on PSMSL tide-gauge records are twice as large as the standard deviations of differences between the land-uplift model and rates from NMA tide-gauge data.

The last two columns of Table 2 list coastal averages of VLM and uncertainties defined in Equation (1), where both quantities represent values averaged over tide gauges. We notice that the mean uncertainties when using 20 Hz CS2 observations are almost half of the mean uncertainties when using 1 Hz CS2 sea-level anomalies. The NKG uplift model has a coastal average of 2.8 mm/year over all 20 tide gauges. $VLM_{1HzPSMSL}$ shows a coastal average of 4.4 mm/year and VLM_{1HzNMA} of 2.4 mm/year. VLM rates based on 20 Hz CS2 data show coastal averages of 5.5 mm/year ($VLM_{20HzPSMSL}$) and 3.4 mm/year ($VLM_{20HzNMA}$). We used the Welch's unequal variances *t* test [29] (two-tailed, with $\alpha = 0.05$) to check whether the coastal averages of estimated VLM rates are significantly different from the coastal average of the NKG uplift model rates. The average rates of our four VLM solutions along the Norwegian coast were not significantly different from the coastal average of the NKG uplift model at the 95% level. Though the coastal averages of VLM rates calculated with PSMSL data ($VLM_{1HzPSMSL}$ and $VLM_{20HzPSMSL}$) differ more from the coastal average of the NKG uplift model, they were not significantly different. This is most likely due to the high spread of the PSMSL-based VLM rates, and the fact that two most different estimates may pass the Welch's unequal variances *t* test if one of the two data sets has a large variance. The mean Spearman's rank correlation coefficient between VLM estimates based on PSMSL data and the NKG uplift model is 0.53 when using 1 Hz CS2 data, and 0.46 when using the 20 Hz CS2 observations (Figure 4a,c). Employing NMA tide-gauge records, the mean correlation between VLM rates and the NKG uplift model over all tide gauges is 0.58 and 0.43 for 1 and 20 Hz CS2 data, respectively (Figure 4b,d). The mean correlations calculated for the Norwegian coast are lower than 0.77 obtained by Pfeffer and Allemand [3] at 113 GPS sites. At the same time, they outperform the results by Nerem and Mitchum [2] (0.35 at 33 nearby GPS and DORIS sites) and Ostanciaux et al. [6] (0.40 at 57 GPS sites).

At Vardø, Harstad, Rørvik, Ålesund, Bergen, and Viker, for at least three out of four VLM solutions, differences to the NKG uplift model are maximum 5 mm/year or less. Although most of those tide gauges are inside fjords and land-confined (except Vardø and Viker), they show a good agreement to the NKG uplift model. At Honningsvåg, Hammerfest, Trondheim, Kristiansund, Måløy, Stavanger, and Tregde, the differences to the NKG uplift model range between 2 and 10 mm/year for three or four VLM solutions. Most of these tide gauges are land-confined, except Kristiansund and Tregde. In turn, high discrepancies between the NKG uplift model and VLM rates from CS2 and tide-gauge data are found at both tide gauges that are land-confined and located to the open ocean. For all four solutions, the largest misfits to the NKG uplift model are observed at Trondheim, Heimsjø, and Oscarsborg, all located deeply inside fjords. Leaving out these tide gauges, the coastal average of the NKG uplift model drops from 2.8 to 2.6 mm/year. Excluding Trondheim, Heimsjø, and Oscarsborg from the comparison reduces the minima and standard deviations of differences for all VLM solutions considerably (see lower part of Table 2). A decrease in the coastal averages of estimated VLM rates is noted as well as reduced uncertainties. Unlike the mean values of differences calculated over all tide gauges, the mean values after excluding Trondheim, Heimsjø, and Oscarsborg are all positive, implying that all VLM solutions have consistently smaller rates than the observations in the NKG uplift model reflect. $VLM_{1HzPSMSL}$ and VLM_{1HzNMA} differ on average 1.4 and 1.5 mm/year from the NKG uplift model, respectively. $VLM_{20HzPSMSL}$ differs on average 0.1 mm/year from the NKG uplift model and $VLM_{20HzNMA}$ 0.3 mm/year. The agreement of mean values between differences of estimated VLM rates and the NKG uplift model is also reflected in the agreement between their coastal averages. VLM rates based on 1 Hz CS2 data show coastal averages of 1.2 mm/year ($VLM_{1HzPSMSL}$) and 1.1 mm/year (VLM_{1HzNMA}), while estimates of VLM based on 20 Hz data have coastal averages of 2.5 mm/year ($VLM_{20HzPSMSL}$) and 2.3 mm/year ($VLM_{20HzNMA}$).

Table 1. Number of available CS2 SARIn observations in CS2 boxes and the overall agreement (mean Spearman's rank correlation coefficient and mean standard deviation) between CS2 and tide-gauge time series at 20 Norwegian tide gauges.

	No. of CS2 Observations			Mean Corr.	Mean Std (cm)	Mean Corr.	Mean Std [cm]
CS2	**Min**	**Max**	**Mean**	**PSMSL**		**NMA**	
1 Hz	24	402	218	0.53	17.55	0.82	11.89
20 Hz	269	6738	3359	0.50	16.70	0.77	12.12

Table 2. Statistics of NKG2016LU_abs signal as well as statistics of differences between NKG2016LU_abs and VLM rates based on CS2 observations and tide-gauge data along the Norwegian coast in mm/year. The upper part of the table shows the statistics over all 20 tide gauges, while the lower part shows the statistics excluding Trondheim, Heimsjø, and Oscarsborg. The last two columns represent the coastal averages and uncertainties (defined in Equation (1) for estimated VLM rates and adopted from Olsson et al. [28] for NKG2016LU_abs) calculated over tide gauges.

	Min	Max	Mean	Std	Coastal Average	Uncertainty
NKG2016LU_abs	1.3	4.7	-	1.1	2.8	0.6
NKG2016LU_abs - . . .						
$VLM_{1HzPSMSL}$	−23.2	16.3	−1.5	11.0	4.4	10.8
VLM_{1HzNMA}	−13.9	8.1	0.4	4.8	2.4	6.2
$VLM_{20HzPSMSL}$	−23.2	14.5	−2.7	10.0	5.5	6.2
$VLM_{20HzNMA}$	−10.5	6.5	−0.5	4.1	3.4	3.2
NKG2016LU_abs [a]	1.3	4.3	-	1.0	2.6	0.6
NKG2016LU_abs - . . . [a]						
$VLM_{1HzPSMSL}$	−12.3	16.3	1.4	8.7	1.2	9.5
VLM_{1HzNMA}	−3.9	8.1	1.5	3.5	1.1	5.3
$VLM_{20HzPSMSL}$	−13.1	14.5	0.1	7.7	2.5	4.4
$VLM_{20HzNMA}$	−5.5	6.5	0.3	3.4	2.3	2.3

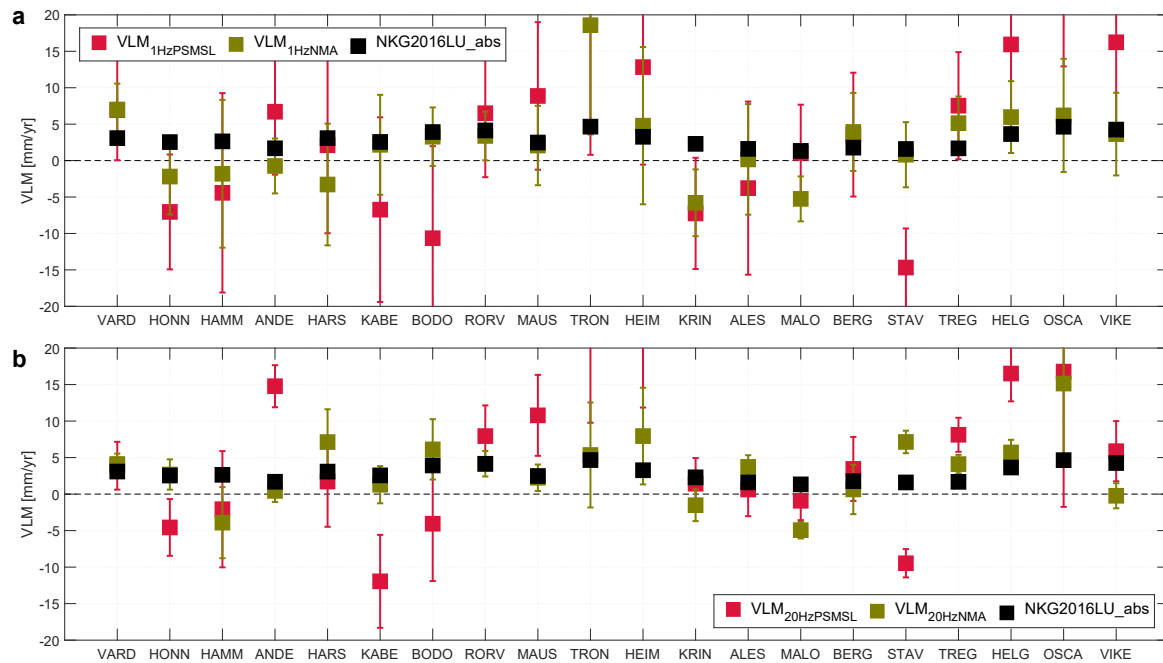[a] Trondheim, Heimsjø, and Oscarsborg were excluded.

Figure 3. Rates of VLM at 20 Norwegian tide gauges. Black squares represent rates from NKG2016LU_abs, while red and green squares represent VLM calculated from tide-gauge data provided by PSMSL and NMA, respectively, and CS2 sea-level anomalies. (**a**) VLM rates based on 1 Hz CS2 time series. (**b**) VLM rates based on 20 Hz CS2 time series. The size of squares corresponds to 2 mm/year. The error bars indicate the associated uncertainties σ calculated by Equation (1), taking into account serial correlations in the measurements. The uncertainty of VLM rates from NKG2016LU_abs is 0.6 mm/year [28].
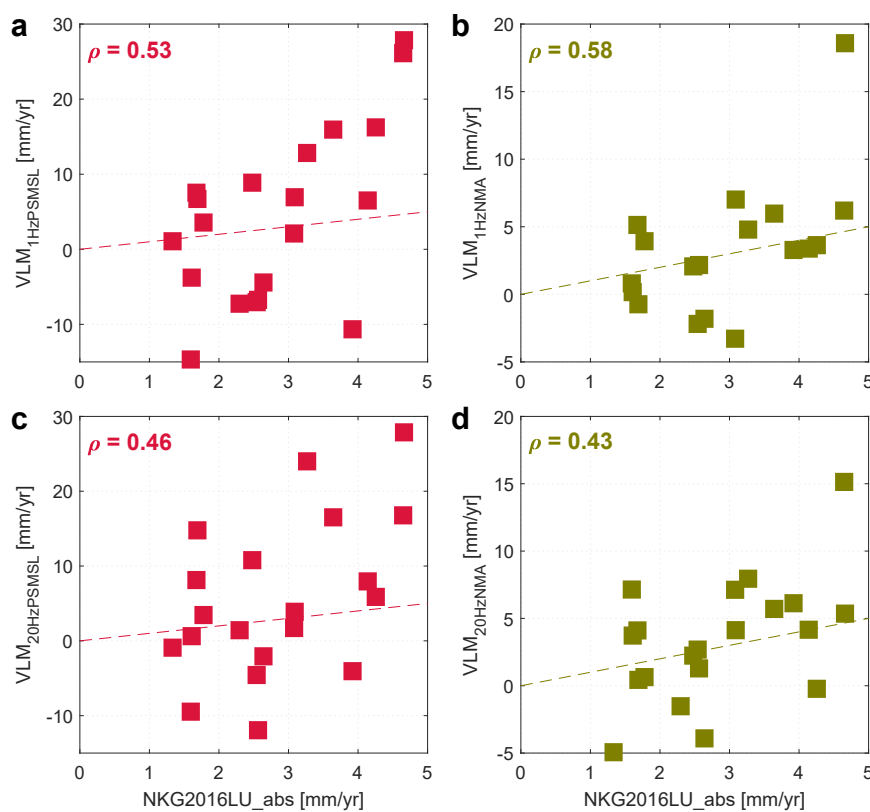

Figure 4. Comparison of estimated VLM rates with rates from NKG2016LU_abs. Spearman's rank correlation coefficient ρ is shown, which was computed over all 20 tide gauges.

4. Summary and Discussion

We have assessed VLM at 20 tide gauges along the Norwegian coast by computing linear trends of differences between CS2 and tide-gauge time series for the period 2010–2018. Two tide-gauge data sets have been used: (i) monthly sea-level observations from PSMSL and (ii) 10-min sea-level measurements obtained from NMA. The agreement between the CS2 and tide-gauge time series is given in Table 1. The resulting VLM rates with associated uncertainties are shown in Figure 3 and Supplementary Materials Table S1, while the statistics of the comparison with the NKG uplift model is given in Table 2 and Figure 4.

The 1 Hz CS2 data agree better with the tide-gauge time series than the 20 Hz data in terms of mean correlations. The agreement between the 20 Hz CS2 data and tide-gauge data from NMA (mean standard deviation of 12.1 cm and mean correlation of 0.77) represents encouraging improvements compared to the results in Idžanović et al. [22]. For the same 20 tide gauges, they obtained a mean standard deviation of 14.7 cm and a mean correlation of 0.64 using standard CS2 corrections and the simple threshold retracker. Our results demonstrate that the SAMOSA 2 retracker has improved the coastal performance compared to the empirical retracker. Furthermore, the tide-gauge data with 10-min sampling interval agree significantly better with CS2 measurements than the monthly PSMSL time series. The smaller correlation and higher standard deviation between CS2 and the PSMSL time series (see Table 1) can be explained by most different sampling rates. The 1 or 20 Hz sampling frequencies of CS2 imply that the altimetry observations include ocean signals, which are averaged to nearly zero in the monthly tide-gauge data. Consequently, differential ocean signals may be introduced in the series of differences between CS2 and the monthly tide-gauge data. This, in turn, may lead to less accurate VLM estimates and a possibly poorer fit to the NKG uplift model.

Our results are encouraging and suggest that CS2 in combination with the high-frequency NMA tide-gauge data can reflect the coastal average of VLM over 20 tide gauges along the Norwegian coast. At Honningsvåg, Kabelvåg, Rørvik, Mausund, and Viker, are differences between VLM rates based on NMA data and the NKG uplift model within the uncertainty of the land-uplift model. In addition, the agreement between the NKG uplift model and NMA-based VLM solutions indicates that there are no systematic errors in the Norwegian national sea-level observing system. Furthermore, the results obtained along the coast demonstrate that altimetry in combination with tide-gauge data can be used to determine VLM at tide gauges where there are no nearby GPS receivers nor rates available from a VLM model.

In general, the spread of rates from CS2 and tide gauges is larger than that of the NKG uplift model. This is especially notable for the PSMSL-based VLM rates, where the combination of CS2 with PSMSL tide-gauge records does not observe the VLM at some tide gauges. However, the NMA-based VLM solutions show a much smaller spread of differences to the NKG uplift model and a high spatial correlation. The comparison between estimated VLM rates and the NKG uplift model indicates that largest differences occur at tide gauges with an insufficient number of CS2 observations, i.e., at Trondheim, Heimsjø, and Oscarsborg. Excluding those tide gauges, the NKG uplift model shows a coastal average of 2.6 mm/year. Omitting Trondheim, Heimsjø, and Oscarsborg from the comparison, the standard deviations of differences decrease along with a significant drop in the mean uncertainties. In addition, eliminating Trondheim, Heimsjø, and Oscarsborg, the largest improvement is found for the PSMSL-based VLM solutions. Combining 1 and 20 Hz data with tide-gauge data provided by NMA gives coastal averages of 1.1 and 2.3 mm/year, respectively. VLM rates calculated combining tide-gauge measurements from PSMSL with 1 and 20 Hz CS2 data show coastal averages of 1.2 and 2.5 mm/year, respectively. In case of omitting the problematic tide gauges, we note a stronger dependence of VLM estimates to the CS2 sampling, and a better fit of VLM rates based on 20 Hz data to the NKG uplift model.

Different OT corrections applied to CS2 (FES2004) and tide-gauge measurements (OT corrections provided by NMA) are possible reasons for the misfit between the NKG uplift model and calculated VLM rates at some tide gauges. Particularly at Hammerfest, Trondheim, Heimsjø, and Kristiansund,

discrepancies between signal standard deviations of FES2004 and local OT corrections within CS2 boxes are ranging from 6.7 to 28.5 cm. At these stations, we also find the largest differences to the NKG uplift model. In addition, the CS2 sea-surface observations come from multiple tracks within the CS2 boxes. Potential MSS errors will appear as SLA offsets between individual tracks, possibly introducing SLA errors [30] and, in turn, affecting the VLM estimation. Especially at the coast, it becomes a problem where no observations are available, and the MSS is simply extrapolated. In general, the observed discrepancies between altimetric sea-level anomalies and tide-gauge sea level, and in turn the large spread of estimated VLM rates not seen in the NKG uplift model, might be due to an insufficient number of CS2 observations within CS2 boxes, instrument noise and complex ocean [22] or other coastal processes (e.g., local subsidence not represented by the NKG uplift model).

The estimated errors of VLM rates are strongly dependent on the number of CS2 observations available in each CS2 box. Consequently, mean uncertainty estimates based on 20 Hz data (6.2 mm/year for $VLM_{20HzPSMSL}$ and 3.2 mm/year for $VLM_{20HzNMA}$) are much smaller than those based on 1 Hz data (10.8 mm/year for $VLM_{1HzPSMSL}$ and 6.2 mm/year for VLM_{1HzNMA}). Extension of the CS2 data span would improve the accuracy of the estimated VLM rates [5]. A next step in the VLM estimation from CS2 and tide gauges could be a link of relative VLM between tide gauges, as presented in Kuo et al. [1], using additional conditions and taking advantage of long-term tide-gauge records available in Fennoscandia. In addition, replacing the standard CS2 OT correction with a local one, as demonstrated in Idžanović et al. [22], could possibly lead to a better agreement of estimated VLM rates with the NKG uplift model. Especially at tide gauges, where discrepancies between standard and local OT corrections are large. Furthermore, expanding the estimation of VLM rates using CS2 and tide-gauge measurements to the Baltic Sea region will be considered in the future, where the VLM signal reaches values up to ∼10 mm/year.

Author Contributions: Conceptualization, M.I.; Methodology, M.I.; Software, M.I.; Validation, M.I.; Formal Analysis, M.I., C.G., K.B., and O.B.A.; Investigation, M.I.; Resources, M.I., C.G., K.B., and O.B.A.; Data Curation, M.I.; Writing—Original Draft Preparation, M.I.; Writing—Review & Editing, C.G., K.B., and O.B.A.; Visualization, M.I.; Supervision, C.G., K.B., and O.B.A.; Project Administration, C.G. and K.B.; Funding Acquisition, C.G., K.B., and O.B.A.

References

1. Kuo, C.Y.; Shum, C.K.; Braun, A.; Mitrovica, J.X. Vertical crustal motion determined by satellite altimetry and tide gauge data in Fennoscandia. *Geophys. Res. Lett.* **2004**, *31*, L01608. [CrossRef]
2. Nerem, R.S.; Mitchum, G.T. Estimates of vertical crustal motion derived from differences of TOPEX/POSEIDON and tide gauge sea level measurements. *Geophys. Res. Lett.* **2002**, *29*, 40-1–40-4. [CrossRef]
3. Pfeffer, J.; Allemand, P. The key role of vertical land motions in coastal sea level variations: A global synthesis of multisatellite altimetry, tide gauge data and GPS measurements. *Earth Planet. Sci. Lett.* **2016**, *439*, 39–47. [CrossRef]
4. Fenoglio-Marc, L.; Dietz, C.; Groten, E. Vertical Land Motion in the Mediterranean Sea from Altimetry and Tide Gauge Stations. *Mar. Geod.* **2004**, *27*, 683–701. [CrossRef]
5. Kuo, C.-Y.; Shum, C.K.; Braun, A.; Cheng, K.-C.; Yuchan, Y. Vertical Motion Determined Using Satellite Altimetry and Tide Gauges. *Terr. Atmos. Ocean. Sci.* **2008**, *19*, 21–35. [CrossRef]

6. Ostanciaux, É.; Husson, L.; Choblet, G.; Robin, C.; Pedoja, K. Present-day trends of vertical ground motion along the coast lines. *Earth-Sci. Rev.* **2012**, *110*, 74–92. [CrossRef]

7. Breili, K.; Simpson, M.J.R.; Nilsen, J.E.Ø. Observed Sea-level Changes along the Norwegian Coast. *J. Mar. Sci. Eng.* **2017**, *5*, 29. [CrossRef]

8. Wingham, D.J.; Francis, C.R.; Baker, S.; Bouzinac, C.; Brockley, D.; Cullen, R.; de Chateau-Thierry, P.; Laxon, S.W.; Mallow, U.; Mavrocordatos, C.; et al. CryoSat: A mission to determine the fluctuations in Earth's land and marine ice fields. *Adv. Space Res.* **2006**, *37*, 841–871. [CrossRef]

9. Idžanović, M.; Ophaug, V.; Andersen, O.B. The coastal mean dynamic topography in Norway observed by CryoSat-2 and GOCE. *Geophys. Res. Lett.* **2017**, *44*, 5609–5617. [CrossRef]

10. Ophaug, V.; Breili, K.; Gerlach, C. A comparative assessment of coastal mean dynamic topography in Norway by geodetic and ocean approaches. *JGR Oceans* **2015**, *120*, 7807–7826. [CrossRef]

11. Vestøl, O.; Ågren, J.; Steffen, H.; Kierulf, H.; Lidberg, M.; Oja, T.; Rüdja, A.; Kall, T.; Saaranen, V.; Engsager, K.; et al. NKG2016LU, an improved postglacial land uplift model over the Nordic-Baltic region. In Proceedings of the NKG Joint WG Workshop on Postglacial Land Uplift Modelling, Gävle, Sweden, 1–2 December 2016.

12. European Space Agency. Geographical Mode Mask. 2018. Available online: https://earth.esa.int/web/guest/-/geographical-mode-mask-7107 (accessed on 25 January 2018).

13. Benveniste, J.; Ambrózio, A.; Restano, M.; Dinardo, S. SAR processing on demand service for CryoSat-2 and Sentinel-3 at ESA G-POD. In *Geophysical Research Abstracts, EGU2016-13084, 2016 EGU General Assembly, Vienna, Austria, 17–22 April 2016*; EGU: Göttingen, Germany, 2016; Volume 18.

14. Ray, C.; Martin-Puig, C.; Clarizia, M.P.; Ruffini, G.; Dinardo, S.; Gommenginger, C.; Benveniste, J. SAR altimeter backscattered waveform model. *IEEE Trans. Geosci. Remote Sens.* **2016**, *53*, 911–919. [CrossRef]

15. Armitage, T.W.K.; Davidson, M.W.J. Using the interferometric capabilities of the ESA CryoSat-2 mission to improve the accuracy of sea ice freeboard retrievals. *IEEE Trans. Geosci. Remote Sens.* **2014**, *52*, 529–536. [CrossRef]

16. Abulaitijiang, A.; Andersen, O.B.; Stenseng, L. Coastal sea level from inland CryoSat-2 interferometric SAR altimetry. *Geophys. Res. Lett.* **2015**, *42*, 1841–1847. [CrossRef]

17. Andersen, O.B.; Stenseng, L.; Piccioni, G.; Knudesn, P. The DTU15 MSS (Mean Sea Surface) and DTU15LAT (Lowest Astronomical Tide) reference surface. In Proceedings of the ESA Living Planet Symposium 2016, Prague, Czech Republic, 9–13 May 2016.

18. Komjathy, A.; Born, G.H. GPS-based ionospheric corrections for single frequency radar altimetry. *J. Atmos. Sol.-Terr. Phys.* **1999**, *61*, 1197–1203. [CrossRef]

19. Lyard, F.; Lefevre, F.; Letellier, T.; Francis, O. Modelling the global ocean tides: Modern insights from FES2004. *Ocean Dyn.* **2006**, *56*, 394–415. [CrossRef]

20. Carrère, L.; Lyard, F. Modeling the barotropic response of the global ocean to atmospheric wind and pressure forcing—Comparisons with observations. *Geophys. Res. Lett.* **2003**, *30*, 1275. [CrossRef]

21. Dee, D.P.; Uppala, S.M.; Simmons, A.J.; Berrisford, P.; Poli, P.; Kobayashi, S.; Andrae, U.; Balmaseda, M.A.; Balsamo, G.; Bauer, P.; et al. The ERA-Interim reanalysis: Configuration and performance of the data assimilation system. *Q. J. R. Meteorol. Soc.* **2011**, *137*, 553–597. [CrossRef]

22. Idžanović, M.; Ophaug, V.; Andersen, O.B. Coastal sea level from CryoSat-2 SARIn altimetry in Norway. *Adv. Space Res.* **2018**, *62*, 1344–1357. [CrossRef]

23. Koch, K.-R. *Parameter Estimation and Hypothesis Testing in Linear Models*; Springer: Berlin, Germany, 1999; pp. 271–309.

24. Holgate, S.J.; Matthews, A.; Woodworth, P.L.; Rickards, L.J.; Tamisiea, M.E.; Bradshaw, E.; Foden, P.R.; Gordon, K.M.; Jevrejeva, S.; Pugh, J. New data systems and products at the Permanent Service for Mean Sea Level. *J. Coast. Res.* **2013**, *29*, 493–504. [CrossRef]

25. Wilks, D.S. *Statistical Methods in the Atmospheric Sciences*; International Geophysics Series; Academic Press: San Diego, CA, USA, 2006; Volume 59, pp. 131–177.

26. Kierulf, H.P.; Steffen, H.; Simpson, M.J.R.; Lidberg, M.; Wu, P.; Wang, H. A GPS velocity field for Fennoscandia and a consistent comparison to glacial isostatic adjustment models. *JGR Solid Earth* **2014**, *119*, 6613–6629. [CrossRef]

27. Kaufman, G. *Program Package ICEAGE*, version 2004; Manuscript; Institut für Geophysik, Universität Göttingen: Göttingen, Germany, 2004; 40p.

28. Olsson, P.-A.; Breili, K.; Ophaug, V.; Steffen, H.; Bilker-Koivula, M.; Nilsen, E.; Oja, T.; Timmen, L. Postglacial gravity change in Fennoscandia—Three decades of repeated absolute gravity observations. *Geophys. J. Int.* **2019**, *217*, 1141–1156. [CrossRef]

29. Welch, B.L. The generalization of "Student's" problem when several different population variances are involved. *Biometrika* **1947**, *34*, 28–35. [CrossRef] [PubMed]

30. Calafat, F.M.; Cipollini, P.; Bouffard, J.; Snaith, H.; Féménias, P. Evaluation of new CryoSat-2 products over the ocean. *Remote Sens. Environ.* **2017**, *191*, 131–144. [CrossRef]